Available online at www.sciencedirect.com
SCIENCE DIRECT
Biochimica et Biophysica Acta 1720 (2005) 99–109
BIOCHIMICA ET BIOPHYSICA ACTA
BBA
http://www.elsevier.com/locate/bba

Effects of pH-induced variations of the charge of the transmembrane α-helical peptide Ac-$K_2(LA)_{12}K_2$-amide on the organization and dynamics of the host dimyristoylphosphatidylcholine bilayer membrane

Witold K. Subczynski [a,*], Anna Wisniewska [a,b], Akihiro Kusumi [c], Ronald N. McElhaney [d]

[a] *Department of Biophysics, Medical College of Wisconsin, 8701 Watertown Plank Road, Milwaukee, WI 53226, USA*
[b] *Department of Biophysics, Faculty of Biotechnology, Jagiellonian University, Krakow, Poland*
[c] *Institute for Frontier Medical Sciences, Kyoto University, Shougoin, Kyoto 606-8507, Japan*
[d] *Department of Biochemistry, University of Alberta, Edmonton, Alberta, Canada T6G 2H7*

Received 29 August 2005; received in revised form 23 November 2005; accepted 23 November 2005
Available online 27 December 2005

Abstract

The effects of the transmembrane α-helical peptide Ac-$K_2(LA)_{12}K_2$-amide ($(LA)_{12}$) on the phase transition and dynamics of saturated dimyristoylphosphatidylcholine (DMPC) membranes were investigated at different pH using conventional and saturation-recovery EPR observations of phosphatidylcholine spin labels. At a peptide-to-DMPC ratio of 1/10, the main phase-transition temperature of the DMPC bilayer is decreased by 4.0 °C when measured at pH 7.0, by 1.6 °C when measured at pH 9.5, and not affected when measured at pH 11.5. This reversible pH effect is due to the subsequent neutralization of the positive charges of lysine side chains at both ends of $(LA)_{12}$. Apparent pK_as of the lysine side chain amino groups of $(LA)_{12}$ in DMPC bilayer are 8.6 and ~10.9, as compared with the pK_a value of 10.5 for these groups when lysine is dissolved in water. Saturation-recovery curves as a function of oxygen concentration using phosphatidylcholine spin labels in DMPC bilayer containing $(LA)_{12}$ are always mono-exponential when measured at pH 7.0 and 9.5. This observation is consistent with the hypothesis that the lipid exchange rates among the bulk, boundary, and $(LA)_{12}$-rich regions are faster than 0.5 μs, the electron spin-lattice relaxation time in the presence of molecular oxygen, suggesting that stable oligomers of $(LA)_{12}$ do not form. Neutralization of one lysine side chain positive charge on each end of the peptide significantly decreases the ordering effect of $(LA)_{12}$ on the lipid hydrocarbon chains, while its effect on the reorientational motion of terminal groups of lipid hydrocarbon chains is rather moderate. It does not affect the local diffusion-solubility product of oxygen measured in the DMPC-$(LA)_{12}$ membrane interior.

Keywords: Pulse EPR; Spin labeling; α-Helical transmembrane peptide; Model membrane; Oxygen transport

1. Introduction

Proteins are not free-floating in a sea of excess lipids in cellular membranes, and non-random distributions of proteins, protein-rich domains and protein oligomeric structures in particular, play important functional roles in cellular membranes [1,2]. Therefore, an understanding of formation mechanisms of these domains and structures and their molecular organization is a significant issue in the field of membrane biology. The processes of multimerization and assembly of specific membrane proteins and lipids can be subdivided into two categories: those that involve interaction with the cytoskeleton and with peripheral membrane proteins, and those that occur only within the membrane. At a first approximation, these two processes are separable. We are concerned with the second category of processes, i.e., formation and molecular organization of membrane–protein oligomers and protein-rich domains within the membrane (without interaction with cytoskeleton elements).

The synthetic peptide Ac-$K_2GL_{24}K_2A$-amide (P_{24}) and its analogues have been successfully utilized as a model of the hydrophobic transmembrane α-helical segments of integral

* Corresponding author. Tel.: +1 414 456 4038; fax: +1 414 456 6512.
E-mail address: subczyn@mcw.edu (W.K. Subczynski).

0005-2736/$ - see front matter © 2005 Elsevier B.V. All rights reserved.
doi:10.1016/j.bbamem.2005.11.014

membrane proteins (see refs. [3,4]). These peptides contain a long sequence of hydrophobic and strongly α-helical-promoting leucine residues capped at both the N- and C-termini with two positively charged, relatively polar lysine residues. Moreover, the normally positively charged N-terminus and the negatively charged C-terminus have both been blocked in order to provide a symmetrical tetracationic peptide which evenly anchors the ends of the peptide at both sides of the bilayer membrane and inhibits lateral aggregation of the peptide via mutual charge repulsion [5]. A wide variety of approaches have shown that this family of peptides does form very stable α-helices that insert into phosphatidylcholine (PC) and phosphatidylethanolamine model membranes perpendicular to the bilayer surface with the N- and C-termini exposed to the aqueous environment near the bilayer surface [5–11].

We have previously investigated the molecular organization and dynamics of phospholipid model membranes containing the transmembrane α-helical peptides Ac-$K_2L_{24}K_2$-amide (L_{24}) [12], Ac-$K_2A_{24}K_2$-amide (A_{24}) [13] and Ac-$K_2(LA)_{12}K_2$-amide ($(LA)_{12}$) [14] using EPR spectroscopy and spin-labeling techniques. All three peptides form α-helices in methanol and exist as a transmembrane α-helix when incorporated into phospholipids in the absence of water. When water is added, both L_{24} [15–19] and $(LA)_{12}$ [20–22] maintain stable transmembrane associations with various phospholipid bilayers. A_{24}, however, partitions strongly into the aqueous phase, where it exists primarily in a non-α-helical conformation and interacts only weakly with the lipid bilayer due to the insufficient hydrophobicity of the polyalanine core [13].

Conventional EPR spectra, as well as saturation–recovery curves measured both in the presence and the absence of molecular oxygen, showed that, in the case of L_{24} as well as $(LA)_{12}$, phosphatidylcholine spin labels (*n*-PCs) detect the existence of a single homogenous environment. This result indicates that the peptides as well as phospholipids in 1-palmitoyl-2-oleoylphosphatidylcholine (POPC)-L_{24} (or $(LA)_{12}$) membranes are likely to be undergoing fast translational diffusion up to 10 mol% peptide and that the exchange rate of lipids among the bulk, boundary, and L_{24} (or $(LA)_{12}$) cluster regions are fast. Molecular dynamics simulations indicate that, in the liquid-crystalline phase, 10–12 molecules of phosphatidylcholine are required to surround a transmembrane α-helical peptide [15]. Thus, L_{24} (or $(LA)_{12}$) must form L_{24}-rich (or $(LA)_{12}$-rich) regions at 10 mol%, but these regions must form and disperse rapidly (in a time scale shorter than 0.1 μs). This conforms to the conventional EPR spin-label time scale and the electron spin-lattice relaxation time scale in the presence of molecular oxygen. These results have led us to inquire why both peptides, L_{24} and $(LA)_{12}$, do not form larger aggregates with lifetimes longer than 0.1 μs. High peptide-POPC miscibility may be due to the four lysine groups, which place two positive charges on each side of the membrane in the peptide. These repulsive charges may be responsible for preventing aggregation of L_{24} and $(LA)_{12}$.

In our previous work, we paid close attention to the differences in the organization of the hydrophobic peptide surface of L_{24}, $(LA)_{12}$ and A_{24}, keeping the same two charged lysine groups on each end of the peptide. The polyleucine hydrophobic core of L_{24} and the polyalanine hydrophobic core of A_{24} can be approximated by a hard-surfaced smooth cylinder because of the tight packing of the leucine and alanine side chains. In contrast, the hydrophobic core of $(LA)_{12}$ resembles a cylinder with a brush-like surface, where the leucine side chains are separated by the small methyl groups of the alanine side chains. Because of that, the leucine side chains obtain additional motional freedom and the ability to protrude between the phospholipid hydrocarbon chains. The frequency of gauche-trans isomerization of the hydrocarbon chains and the concentration of vacant pockets (voids) in the lipid bilayer are thus reduced, which decreases oxygen transport.

In the present study, we focused on the role of the charged dilysine terminae of $(LA)_{12}$ in its interaction with PC bilayers by neutralizing these charges at high pH. We chose $(LA)_{12}$ because of the stronger effect it has on membrane properties as compared with L_{24} and A_{24}. Additionally, instead of POPC, we chose the dimyristoylphosphatidylcholine (DMPC) lipid bilayer containing saturated hydrocarbon chains in order to study the effect of the peptide on membrane main-phase transition. Indeed, we found that the charge of this peptide has a significant effect on the dynamics and organization of DMPC bilayers.

2. Materials and methods

2.1. Materials

The peptide Ac-$K_2(LA)_{12}K_2$-amide ($(LA)_{12}$) was synthesized by the Protein/Nucleic Acid Shared Facility (Medical College of Wisconsin, Milwaukee, WI). 1-Palmitoyl-2-(*n*-doxylstearoyl)-L-α-phosphatidylcholines (*n*-PC, where $n=5$, 10, 12, and 16), and DMPC were obtained from Avanti Polar Lipids, Inc. (Alabaster, AL).

2.2. Preparation of DMPC-$(LA)_{12}$ membranes

The membranes used in this work were multilamellar dispersions of DMPC containing 1 mol% *n*-PC and 1, 3, or 9.1 mol% $(LA)_{12}$. Briefly, these membranes were prepared by the following method [12,14]. A chloroform solution of DMPC and *n*-PC (containing $0.3–1\times10^{-5}$ mol of lipids) and a methanol solution of $(LA)_{12}$ were mixed to attain the desired lipid-to-peptide ratio, the solvent was evaporated with a stream of nitrogen, and the lipid film on the bottom of the test tube was thoroughly dried under reduced pressure (about 0.1 mm Hg) for 12 h. A buffer solution (0.5 mL) was added to the dried film at 40 °C and vortexed vigorously. The following buffers were used: 10 mM PIPES with 150 mM NaCl for pH 7.0–7.2; 0.1 M boric acid for pH 8.0–10.2; and 0.1 CAPS for pH 11.0–11.5. All buffers were prepared at 25 °C and no temperature correction was made. To ensure that peptide molecules were anchored at both sides of the membrane, all preparations of liposomes (from dry lipids) were made first at pH 7.0 where the lysine side-chain amino groups are charged. For measurements at higher pH, the liposome suspension was pelleted, excess buffer was removed, and new buffer (0.5 mL) was added. To ensure that the buffer trapped inside the liposomes was also changed to the new buffer, the liposome suspension was frozen in liquid nitrogen and reheated to 25 °C. These procedures (pelleting and adding a new buffer) were repeated three times. Suspension of DMPC membranes (without peptide) prepared directly at high pH, or with the use of the procedure described above, showed the same phase-transition temperature and the same membrane characteristics.

2.3. Conventional EPR and phase transition

The lipid dispersion (DMPC or DMPC-$(LA)_{12}$ membranes) was centrifuged briefly and the loose pellet (~20% lipid w/w) was used for EPR measurements. The sample was placed in a 0.9 mm i.d. gas-permeable TPX capillary [23]. The capillary was placed inside the EPR Dewar insert and equilibrated with nitrogen gas, which was also used for temperature control. The sample was thoroughly deoxygenated at a temperature above the phase-transition temperature of the lipid bilayer to obtain the correct lineshape. This is especially important near the phase-transition temperature, because the oxygen concentration-diffusion product changes abruptly at the phase transition of the membrane [24–26]. EPR spectra were obtained with an X-band Varian E-109 spectrometer with an E-231 Varian multipurpose cavity (rectangular TE_{102} mode). For phase-transition measurements, the temperature was regulated by passing the nitrogen gas through the coil placed in a water bath, and was monitored using a copper-constantan thermocouple that was placed in the sample just above the active volume of the cavity [27]. Temperature was regulated to better than 0.1 °C (this was possible because the temperature range used was close to room temperature). Temperature was always lowered by adding a small amount of cold water to the water bath with rapid agitation, permitting a very low rate of temperature change (2 °C/h) in our measurements. Special care was taken not to raise the temperature during the cooling experiment. It was shown [27] that when the nitroxide moiety is attached at the C16 position in the alkyl chain of the lipid spin label (nitroxide fragment located in the center of the DMPC bilayer) the EPR gave very similar results to the DSC measurements. In all measurements of the main phase transition, the 16-PC spin label was used at 1 mol% concentration.

2.4. Saturation-recovery EPR

The spin-lattice relaxation times (T_1s) of spin labels were determined by analyzing the saturation-recovery signal of the central line obtained by short-pulse saturation-recovery EPR at X-band [26,28–30]. Details for measurements with peptides are described in our earlier papers [12,14].

The bimolecular collision rate between oxygen (a fast relaxing species) and the nitroxide spin-label (a slow relaxing species) placed at specific locations in the membrane was evaluated in terms of an oxygen transport parameter ($W(x)$). $W(x)$ was defined as

$$W(x) = T_1^{-1}(\mathrm{air}, x) - T_1^{-1}(N_2, x), \quad (1)$$

where the T_1s are the spin-lattice relaxation times of the nitroxide in samples equilibrated with atmospheric air and nitrogen, respectively [25,26,31]. $W(x)$ is proportional to the product of local translational diffusion coefficient $D(x)$ and the local concentration $C(x)$ of oxygen at a "depth" x in a lipid bilayer that is equilibrated in atmospheric air:

$$W(x) = AD(x)C(x), \; A = 8ppr_0, \quad (2)$$

where r_0 (about 4.5 Å) is the interaction distance between oxygen and the nitroxide radical spin-label [24,32], and p is the probability that an observable event occurs when a collision occurs and is very close to 1 [23].

3. Results and discussion

3.1. Conventional EPR

Fig. 1 shows a panel of conventional EPR spectra of 5-, 10-, 12-, and 16-PC in fluid phase DMPC membranes containing 0 and 1/10 molar ratio of $(LA)_{12}$ to DMPC at 27 °C. Two sets of spectra in the presence of $(LA)_{12}$ indicate the data obtained at pH 7.0 and 9.5. At both pH values there is no indication of the presence of two components (boundary and bulk components) at any temperature and at any $(LA)_{12}$ concentration employed in the present work. Similarly, one-component EPR spectra were previously observed by us at pH 7.0 in POPC membranes

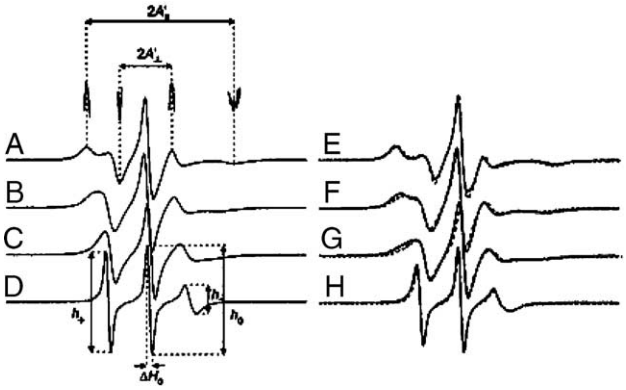

Fig. 1. Panel of EPR spectra of 5-, 10-, 12-, and 16-PC in DMPC membranes in the absence (A, B, C, D) and the presence of 9.1 mol% $(LA)_{12}$ (E, F, G, H) for samples prepared at pH 7.0 (solid lines) and at pH 9.5 (broken lines). Spectra were recorded at 27 °C. Measured values for evaluating the order parameter and rotational correlation times are indicated. The positions of certain peaks were evaluated with a high level of accuracy by recording them at 10 times higher receiver gain and, when necessary, at higher modulation amplitude. The order parameter was calculated according to [42] using the equation $S=0.5407(A'_{||}-A'_{\perp})/a_o$, where $a_o=(A'_{||}+2A'_{\perp})/3$. The rotational correlation time was calculated according to [45] from the linear term of the line with parameter, $\tau_{2B}=6.51\times10^{-10}\Delta H_0[(h_0/h_-)^{1/2}-(h_0/h_+)^{1/2}]$s, and with the quadratic term, $\tau_{2C}=6.51\times10^{-10}\Delta H_0[(h_0/h_-)^{1/2}+(h_0/h_+)^{1/2}-2]$s.

containing $(LA)_{12}$ or L_{24}, leading to the conclusion that the exchange rates of POPC molecules among the bulk, boundary, and peptide cluster regions, are fast (exchange rate to be greater than 10^7 s^{-1}) [12,14].

Our conclusion that $(LA)_{12}$ and L_{24} in their charged forms are well dispersed in fluid state lipid bilayer membranes is compatible with previous studies on the closely related peptide P_{24} in DPPC bilayers with the use of high-sensitivity differential scanning calorimetry (DSC) [9] and deuterium NMR spectroscopy [33]. Also, spin-labeled L_{24} rotates at the rate expected of the transmembrane peptide monomer in a variety of liquid-crystalline PC model membranes ([33]; John D. Stamm and David D. Thomas, personal communication). This miscibility may be due in part to repulsion between the positively charged lysine residues at each end of the peptide molecule. However, single-component EPR spectra were also observed for (LA)-based ditryptophan-terminated WALP peptides incorporated into disaturated PC membranes, indicating that these WALP peptides are also well dispersed in the lipid bilayer even at a peptide-to-lipid ratio of 1/10 [34].

3.2. Main phase transition

The main phase transition of DMPC membranes was monitored by observing the amplitude of the central line of the EPR spectra of 16-PC (h_0 in Fig. 1D). Fig. 2 shows the changes in the normalized signal amplitude of 16-PC in DMPC membranes containing 0, 1, 3, and 9.1 mol% $(LA)_{12}$ recorded at pH 7.0. As the concentration of $(LA)_{12}$ increases, the phase transition shifts toward lower temperatures and the width broadens. The influence of $(LA)_{12}$ on the transition temperature and on the sharpness of the transition depends on the pH of the buffer (compare transition curves in Fig. 2 obtained at pH 7.0

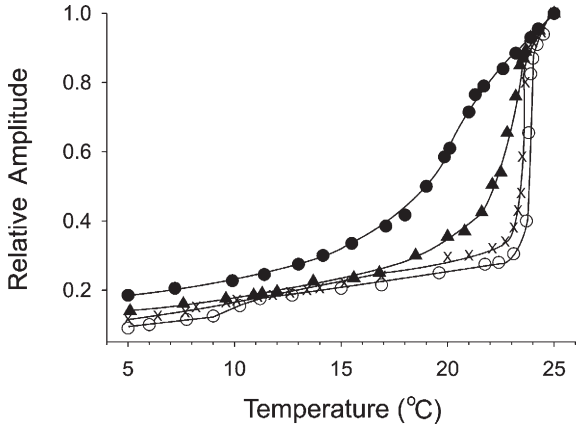

Fig. 2. Normalized intensity of the central peak of the EPR spectra of 16-PC plotted as a function of temperature (cooling experiments), shown as a function of $(LA)_{12}$ concentration in DMPC bilayer: 0 (○), 1 (x), 3 (▲), and 9.1 mol% (●), at pH 7.0. It should be noted that the pretransition that is observed at ~10 °C for pure DMPC bilayer disappears at the presence of 1 mol% $(LA)_{12}$.

and in Fig. 3 obtained at pH 9.5). This difference is due to alterations in interactions of the polar headgroup region of DMPC bilayer with the differently positively charged ends of $(LA)_{12}$ at pH 7.0 and at pH 9.5. Some EPR measurements of the main phase transition were confirmed using DSC measurements. For example, DSC measurements indicated that at pH 7.0 10 mol% $(LA)_{12}$ decreases the phase transition temperature by 5.5 °C. We should point out here that: (1) EPR observations were made from cooling experiments (to make sure that the observed specimen was in thermal equilibrium), whereas DSC measurements were made from the heating experiments, (2) the rate of temperature variation was far smaller in EPR observations than in DSC measurements. These should explain the small differences between EPR and DSC measurements.

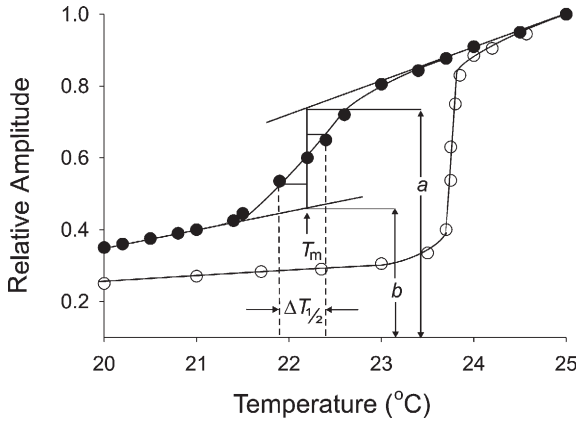

Fig. 3. Normalized intensity of the central peak of the EPR spectra of 16-PC plotted as a function of temperature (cooling experiments), shown as a function of $(LA)_{12}$ concentration in DMPC bilayer: 0 (○) and 9.1 mol% (●), at pH 9.5. Definitions of T_m and $\Delta T_{1/2}$ are shown. T_m is the midpoint temperature at which the normalized EPR signal amplitude equals $(a+b)/2$, where a and b are, respectively, intensities at the given temperatures in the extended linear portions of the upper and lower ends of the transition curve. As the sharpness of the transition, we employed the width $\Delta T_{1/2}$, which is defined by two temperatures at which the EPR signal amplitude is $(a+3b)/4$ and $(3a+b)/4$.

The phase-transition temperature, T_m, and the width of transition, $\Delta T_{1/2}$, were operationally defined from the EPR data as shown in Fig. 3, as was previously done for Raman data [35] and EPR data [27]. These parameters give values close to the transition temperature and width defined by DSC [27,36]. The van't Hoff enthalpy, which can be evaluated from T_m and $\Delta T_{1/2}$ obtained from the EPR experiment, is related to the cooperativity of the phase transition (to the number of molecules in a cooperative unit) [36,37]. The effect of $(LA)_{12}$ on the cooperativity of phase transition (on $\Delta T_{1/2}$) is stronger at pH 7.0 as compared with pH 9.5 and increases with concentration of $(LA)_{12}$ in the DMPC bilayer. Also, at both pH 7.0 and 9.5, the T_m changes linearly with the addition of $(LA)_{12}$ up to 9.1 mol% (data not shown).

3.3. pH profile of the effect of $(LA)_{12}$ on membrane phase transition

Fig. 4 shows pH profiles of the T_m for pure DMPC bilayer and DMPC bilayer containing 9.1 mol% $(LA)_{12}$. It can be seen that the T_m of the pure DMPC membrane does not change with increasing buffer pH from 7.0 up to 10.5, in agreement with other work [38–40]. At higher pH, a decrease in T_m is observed, probably due to the high concentration of OH^- and Na^+ ions which shield the charges of the phosphatidylcholine groups and decrease interaction between the polar headgroups of phospholipids. PCs and other phospholipids also become chemically unstable at pH extremes due to OH^-- and Na^+-catalyzed hydrolysis (McElhaney, unpublished data).

As can be seen from Fig. 4, the main phase-transition temperature of DMPC bilayer is significantly lowered in the presence of 9.1 mol% $(LA)_{12}$ at pH 7.0, as reported previously

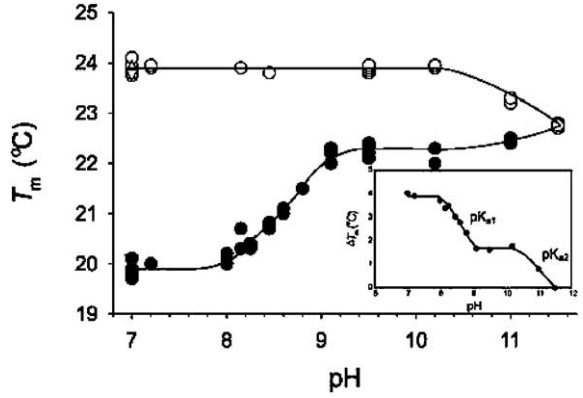

Fig. 4. T_m plotted as a function of pH for DMPC membranes resuspended in appropriate buffer. DMPC membranes contained 0 (○) and 9.1 (●) mol% $(LA)_{12}$. All samples were prepared at pH 7.0 and transferred to a new buffer as described in Materials and methods. To check that this procedure does not affect the membrane properties, membranes from pH 9.5 (Δ, ▲), 10.2 (□, ■), and 11.5 (▽, ▼) were transferred back to pH 7.0 giving the same results as membranes prepared directly at pH 7.0. Open symbols are for DMPC membranes without $(LA)_{12}$ and closed symbols are for DMPC membranes containing 9.1 mol% $(LA)_{12}$. One point in this display indicates one measurement (cooling experiment). We should indicate that for pH 7.0 and 9.5 we performed a minimum of four repetitions. Insert, pH dependence of the differences (ΔT_m) between the phase-transition temperature of pure DMPC membranes and those containing 9.1 mol% $(LA)_{12}$.

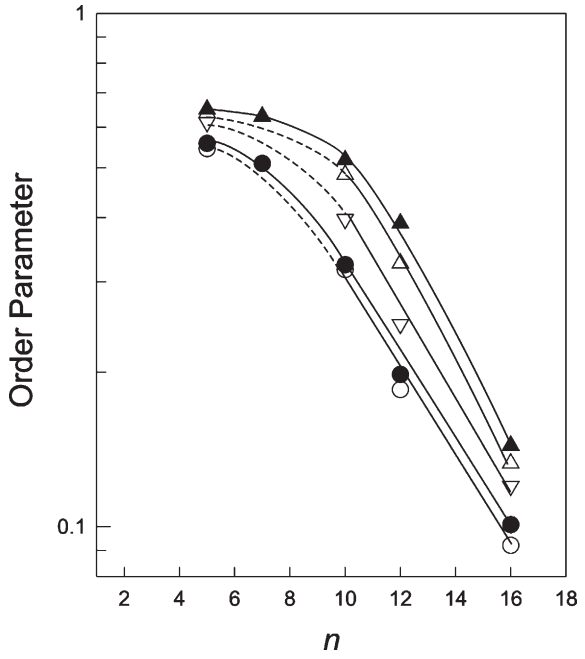

Fig. 5. Profiles of the molecular order parameter (order parameter is plotted in a log scale as a function of nitroxide position (n) along the acyl chain in n-PC) at 35 °C in DMPC membranes (○, 0 mol% $(LA)_{12}$, pH 7.0; Δ, 9.1 mol% $(LA)_{12}$, pH 7.0; ▽, 9.1 mol% $(LA)_{12}$, pH 9.5). Order parameter profiles in POPC membranes at 35 °C and at pH 7.0 in the absence (●) and presence (▲) of 9.1 mol% $(LA)_{12}$ are also shown. Broken lines between the 5th and 10th positions in DMPC membranes were drawn assuming similar changes of the order parameter in DMPC and POPC membranes.

by DSC [10]. Additionally, the effect of $(LA)_{12}$ depends on the pH at which the membrane suspension is prepared. At pH close to 7.0, the phase-transition temperature is lowered to 19.9 °C, and at pH close to 9.5, it is lowered to 22.3 °C, while at pH 11.5, the phase-transition temperature is not affected by the addition of $(LA)_{12}$. The insert in Fig. 4 clearly indicates two midpoints of the T_m change that occur at pH 8.6 and pH ~10.9. This behavior indicates that the four lysine side chain amino groups are ionized at pH 7.0 (two plus charges are present on both ends of the peptide molecule), the two lysine side chain amino groups are ionized at pH 9.5 (one plus charge is present on both ends of the peptide molecule), and that lysine side chains are neutral at pH higher than 11.5. We assume that the $(LA)_{12}$ molecule is essentially symmetric in regard to the disposition of two lysine residues at each end of the helix, and that the two terminal and two anterminal lysine residues at each end of the molecule have similar pK_a values. As can be seen from the results presented in Fig. 4, the pH effect is completely reversible.

According to Chaimovich et al. [41], the apparent pK_a of $(LA)_{12}$ incorporated into a lipid bilayer is the bulk water pH at which the population of charged species equals the population of uncharged species. Assuming the linearity of the effects of charged and uncharged forms of $(LA)_{12}$ on the T_m of DMPC, which was confirmed in this work, the apparent pK_as are indicated by midpoints of the change in the effect of $(LA)_{12}$ on the T_m of DMPC. Thus, the apparent pK_a values for the protonation of the amino groups of the lysine side chain in the DMPC bilayer are 8.6 and ~10.9, as can be clearly seen from the insert in Fig. 4. It should be pointed out that in aqueous solution the pK_a value for the lysine side chain amino groups is 10.5. We speculate that the lysine amino groups more exposed to water phase exhibit higher pK_a value and those located deeper in the membrane exhibit lower pK_a value. Below, we compared other properties of DMPC-$(LA)_{12}$ membranes at pH 7.0 with those at pH 9.5 what gives us the information how amount of the charge on both ends of the peptide molecule affect its interaction with lipid bilayer membranes.

3.4. Effects of $(LA)_{12}$ on alkyl chain order

Fig. 5 shows the profile of the order parameter obtained with 5-, 10-, 12-, and 16-PC in DMPC-$(LA)_{12}$ membranes at 35 °C. The order parameter S was calculated from EPR spectra according to Marsh [42]; $A'_{||}$ and $A'_{\perp}$ were measured directly from the EPR spectra as shown in Fig. 1. In the case of n-PC, S reflects the segmental order parameter of the hydrocarbon chain segment to which the nitroxide fragment is attached. In the model in which the wobbling motion of the segment is treated as Brownian rotational diffusion within the confines of a cone of a semi-cone angle of θ_C, these spatial confines, imposed by the membrane environment, can be described as a square well potential with infinitely high barriers at θ_C [43]. The order parameter can be related to the semi-cone angle θ_C according to the equation [43]:

$$S = \cos h_C(1 + \cos h_C)/2 \quad (3)$$

The changes of the semi-cone angle are summarized in Table 1. The effect of $(LA)_{12}$ on the wobbling motion of lipid molecules at different pH can be clearly indicated in this table. The alkyl chain order increased (and the semi-cone angle decreased) significantly at all depths in the presence of $(LA)_{12}$ and the effect of the peptide measured at pH 7.0 in the saturated DMPC bilayer is slightly smaller than that in the unsaturated POPC bilayer. However, a significant difference is observed between the results at pH 7.0 and at pH 9.5: the ordering effect of the form of $(LA)_{12}$ with one plus charge at each end is weaker than the ordering effect of its form with two plus charges. Again, the pH effect is reversible.

The maximum splitting value ($2A'_{||}$ in Fig. 1) is directly related to the order parameter of the spin label [44] and has been used here as a convenient and easily obtained parameter to monitor differences in the effect of $(LA)_{12}$ on alkyl chain order at different pH. The maximum splitting value increases with the increase of alkyl chain order. Fig. 6 shows the maximum

Table 1
Effect of inclusion of 9.1 mol% $(LA)_{12}$ in DMPC membranes on the semi-cone angle (degree) of n-PC at 35 °C

n-PC	No additions	9.1 mol% $(LA)_{12}$	9.1 mol% $(LA)_{12}$
	pH 7.0	pH 7.0	pH 9.5
5-PC	48.9	42.5	44.4
10-PC	63.9	52.8	58.5
12-PC	73.3	63.3	68.7
16-PC	80.9	77.4	78.5

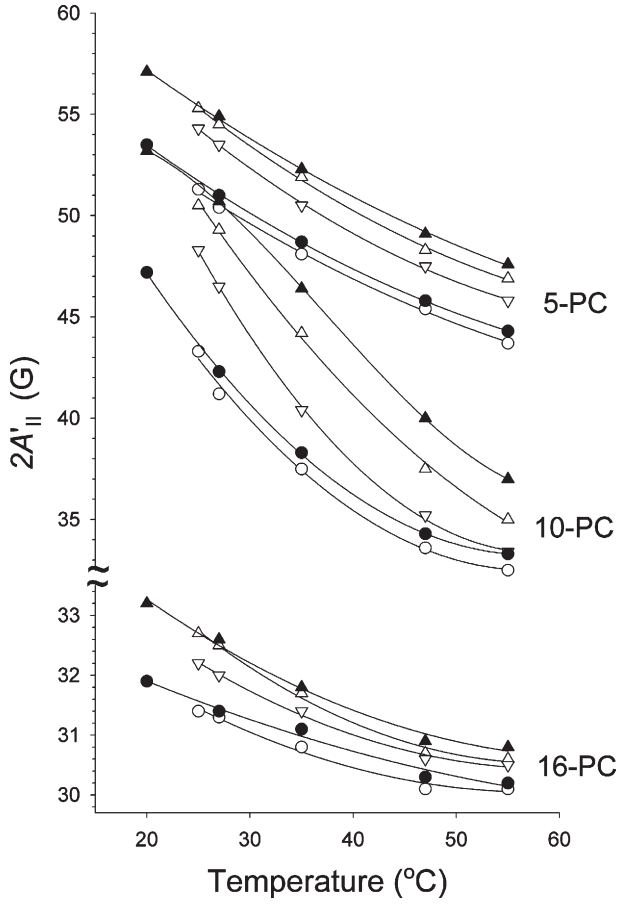

Fig. 6. Maximum splitting values ($2A'_{II}$) of 5-, 10-, and 16-PC in DMPC membranes (○, 0 mol% $(LA)_{12}$, pH 7.0; Δ, 9.1 mol% $(LA)_{12}$, pH 7.0; ▽, 9.1 mol% $(LA)_{12}$, pH 9.5) plotted as a function of temperature. Data obtained in POPC membranes at pH 7.0 in the absence (●) and presence (▲) of 9.1 mol% $(LA)_{12}$ are also shown. For clarity of the display we omitted data for 12-PC. It should be noted that the maximum splitting scale is extended three times for 16-PC as compared with the scale for 5- and 10-PC. Maximum measurement errors are estimated to be 0.25 G.

splitting of *n*-PC spin labels in the DMPC bilayer containing 0 and 9.1 mol% $(LA)_{12}$ at pH 7.0 and 9.5, respectively, as a function of temperature. The values in POPC obtained at pH 7.0 are also presented. It can be seen that the most sensitive spin label for indication of the changes in maximum splitting (order parameter) is 10-PC.

De Planque et al. [34] used conventional EPR and ^{2}H-NMR spectroscopy to investigate the effect of (LA)-based WALP peptides on disaturated PC membranes. The WALP peptides are uncharged and consist of a sequence with alternating leucine and alanine residues, flanked on both sides by two tryptophanes, and with N- and C-termini blocked. WALP peptides incorporated into PC bilayers of comparable thickness exhibit small or no change in hydrophobic chain orientational order. This indicates a similar tendency as observed here that the decrease in the amount of the positive charge on each end of the $(LA)_{12}$ molecule lowers its ordering effect. However, the comparison with WALP peptides has to be made carefully because of the differences in the hydrophobic length.

3.5. Effect of $(LA)_{12}$ on 16-PC reorientational motion

The effective rotational correlation time of 16-PC was obtained by assuming isotropic rotational diffusion of the attached nitroxide ([45], see caption for Fig. 1). The plots of log τ vs. reciprocal temperature shown in Fig. 7 for DMPC membranes are straight lines and the rotational diffusion of the 16-PC nitroxide moiety can be characterized by single activation energy. Addition of peptide decreases the rate of rotational motion of 16-PC and decreases the activation energy of this motion. Moreover, these effects are stronger for the ionized form of the peptide (at pH 7.0) as compared with the effects of the semi-ionized form (at pH 9.5) and this pH effect is reversible. Because of the different slopes of the lines, this difference is more pronounced at higher temperatures.

The rotational diffusion of 16-PC nitroxide moiety in POPC membranes cannot be characterized by single activation energy (plots in Fig. 7 for these membranes are not linear). However, the slopes of the curves of membranes containing $(LA)_{12}$ are lower than those of pure POPC membranes at all temperatures. This means that $(LA)_{12}$ also decreases the activation barrier for rotational diffusion of 16-PC in POPC membranes. However,

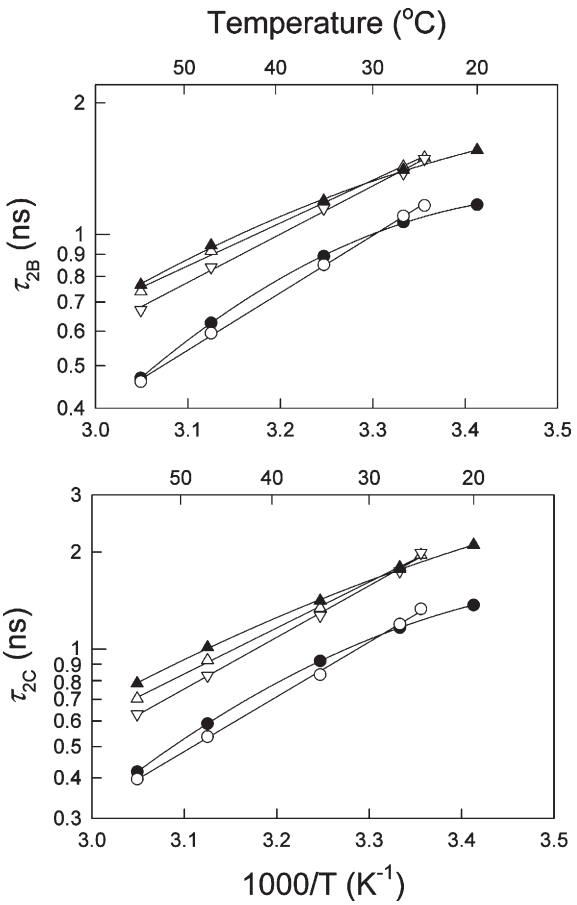

Fig. 7. Effective rotational correlation times, τ_{2B} and τ_{2C}, of 16-PC in DMPC membranes (○, 0 mol% $(LA)_{12}$, pH 7.0; Δ, 9.1 mol% $(LA)_{12}$, pH 7.0; ▽, 9.1 mol% $(LA)_{12}$, pH 9.5) plotted as a function of reciprocal temperature. Data obtained in POPC membranes at pH 7.0 in the absence (●) and presence (▲) of 9.1 mol% $(LA)_{12}$ are also shown.

the difference between the effect of $(LA)_{12}$ in saturated and unsaturated membranes is not as great as for the order parameter. It can be concluded that $(LA)_{12}$ affects membrane fluidity in the center of the lipid bilayer similarly in saturated and unsaturated membranes.

3.6. Saturation–recovery curves indicate fast mixing of the membrane components in DMPC-$(LA)_{12}$ bilayer

Saturation–recovery measurements were performed only at two locations in the DMPC bilayer containing 0 and 9.1 mol% $(LA)_{12}$, for 5-PC (close to the membrane surface) and 16-PC (in the membrane center). Saturation–recovery curves were recorded for samples equilibrated with nitrogen and with mixtures of nitrogen and air (10, 25, and 50% air) at 25 °C, fitted by single, double, and triple exponentials and compared. The results indicated that, for all of the recovery curves obtained in this work, no substantial improvement in the fitting was observed when the number of exponentials was increased from one, suggesting that these recovery curves can be analyzed as single exponentials. The decay time constants were determined with an accuracy of 3%.

We are aware that proving the absence of the strongly immobilized component in conventional EPR spectra is difficult. Previously, we showed that the oxygen transport parameter, $W(x)$, obtained from the saturation–recovery measurements, is a better monitor for distinguishing different membrane domains when the lifetime of domains is longer than $W(x)^{-1}$ [29,46,47]. As we described earlier, the oxygen transport parameter did not show any signs of the presence of two membrane domains when the charged forms of $(LA)_{12}$ or L_{24} (measurements at pH 7.0) were dispersed in POPC membranes even at concentrations as high as 10 mol% [12,14]. Here we also performed measurements of the oxygen transport parameter for DMPC-$(LA)_{12}$ membranes at pH 7.0 and 9.5.

Fig. 8 shows typical saturation–recovery curves for 5-PC in DMPC bilayer containing 9.1 mol% $(LA)_{12}$ and prepared at pH 7.0 and 9.5. As can be seen from the residual, even in the presence of oxygen, all recovery curves could be fitted by a single exponential function and the fits are exceptional. Single-exponential recovery curves were also observed for 16-PC in DMPC membranes without and with $(LA)_{12}$. This indicates the presence of a single homogenous membrane environment at

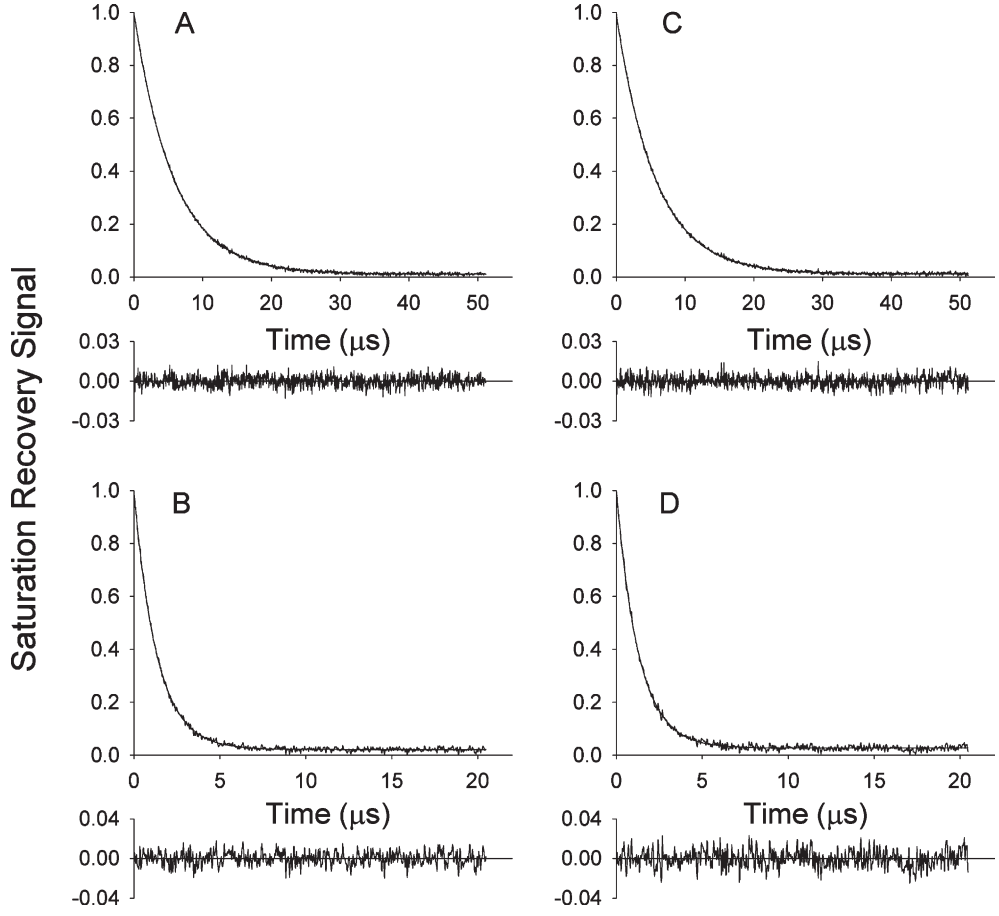

Fig. 8. Representative saturation-recovery signals and fitting curves of 5-PC in DMPC membranes in the presence of 9.1 mol% $(LA)_{12}$ at 25 °C. Panels A and B show results for the sample prepared at pH 7.0 and panels C and D for the sample prepared at pH 9.5. Panels A and C were obtained for samples equilibrated with 100% nitrogen gas. Panels B and D were obtained for samples equilibrated with a gas mixture of 50% air and 50% nitrogen at 25 °C. The solid lines indicate the fit to single exponential curves with recovery times of 5.74 μs for panel A, 1.33 μs for panel B, 5.66 μs for panel C, and 1.29 μs for panel D. The difference between the experimental data and the fitted curve is shown in the lower part of each recovery curve.

both pHs for both forms of $(LA)_{12}$ with two and one positive charge on each end of the molecule in DMPC bilayer. Thus the rates of lipid exchange among the bulk, boundary, and peptide-rich regions are greater than the T_1 relaxation rate (greater than 2×10^6 s^{-1}, because the shortest relaxation time measured in these experiments in the presence of 50% air was 0.5 μs; see ref. [19] for more detail).

The detection of a single homogenous membrane environment for both forms of $(LA)_{12}$ suggests that both forms of the peptide are well dispersed in the DMPC bilayer. We should stress here that the saturation–recovery measurements are sensitive to the processes longer than approximately 0.1 μs. Our conclusion that $(LA)_{12}$ is highly miscible in DMPC bilayer, even when it exists in the less charged form (at pH 9.5), is supported by the work of de Planque et al. [34]. They also concluded, based on observed single-component EPR spectra, that even uncharged WALP peptides are present in liquid-crystalline saturated PC bilayers as monomers. We also performed some saturation-recovery experiments with T-PC (nitroxide moiety located in the polar headgroup region) and 12-PC (nitroxide moiety located close to the membrane center) in POPC membranes containing 0 and 9.1 mol% $(LA)_{12}$ at pH 9.5. All saturation–recovery signals obtained in the absence and presence of molecular oxygen (up to 50% air) in a wide range of temperatures (from 10 to 45 °C) showed mono-exponential behavior indicating fast mixing of membrane components in unsaturated POPC bilayer also containing the $(LA)_{12}$ with one positive charge at each end of the molecule. We direct readers to the General Discussion section where possibilities to detect oligomers of transmembrane α-helical peptides are discussed.

In Fig. 9, T_1^{-1} values for 5- and 16-PC in DMPC membranes with or without 9.1 mol% $(LA)_{12}$ at 25 °C and pH 7.0 and 9.5 are shown as a function of oxygen concentration (in percent air) in the equilibrating gas mixture. All plots of T_1^{-1} for these membranes show a linear dependence on the oxygen concentration between 0 and 50% air. The oxygen transport parameters, $W(x)$, were obtained from the slope of the linear plots in Fig. 9 according to Eq. (1) and are collected in Table 2.

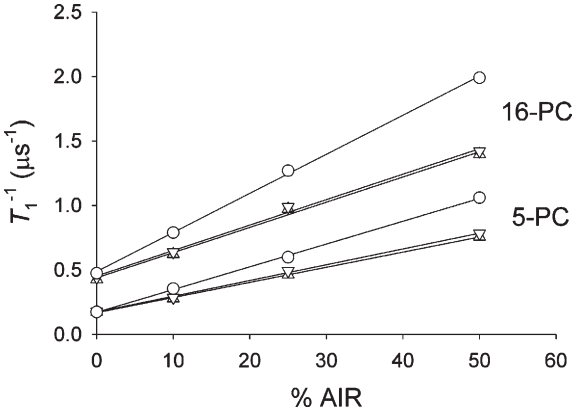

Fig. 9. T_1^{-1} for 5-PC and 16-PC in DMPC membranes containing 0 mol% (○) and 9.1 mol% $(LA)_{12}$ (Δ, ▽) at 25 °C plotted as percent air (v/v) in the equilibrating gas mixture. Samples were prepared at pH 7.0 (Δ) and at pH 9.5 (▽).

Table 2
Oxygen transport parameter values, $W(x)$, for 5-PC and 16-PC in DMPC membranes containing $(LA)_{12}$ at pH 7.0 and 9.5 [a]

Additions ($(LA)_{12}$ mol%)	pH	$W(x)$ values (μs^{-1})	
		5-PC	16-PC
0	7.0	1.76	3.03
9.1	7.0	1.17	1.96
9.1	9.5	1.23	1.97
0 [b]	7.0	1.45	2.80
9.1 [b]	7.0	0.93	1.66

[a] $W(x)$ was obtained with an accuracy better than 10%.
[b] Values for POPC membranes extrapolated to 25 °C from [14]. We also made systematic measurements of the oxygen transport parameter in POPC for T-PC (polar headgroup region) and 12-PC (region close to the membrane center) at pH 9.5 for membrane containing 0 and 9.1 mol% $(LA)_{12}$ in the temperature region 10–45 °C. Obtained values are practically the same as those obtained at pH 7.0 and presented by Subczynski et al. [14].

Results presented in Fig. 9 and Table 2 indicate a large decrease in $W(x)$ by incorporation of $(LA)_{12}$ into the DMPC bilayer, both close to the membrane surface and in the membrane center. The results obtained in the saturated DMPC bilayer are in agreement with those obtained in the unsaturated POPC bilayer, where $(LA)_{12}$ also induced a strong decrease of $W(x)$ across the entire lipid bilayer [14]. Also here the same tendency of the greater effect at pH 7.0 as compared to that at pH 9.5 can be seen. However, the difference is very small (~5%), less than the typical accuracy of measurements of the oxygen transport parameter (~10%).

4. General discussion

To test the hypothesis that charges of dilysine termini are responsible for preventing aggregation of $(LA)_{12}$ in lipid bilayer membranes, first, we studied the effect of $(LA)_{12}$ on membrane properties at high pH and compared them with properties at pH 7.0, at which the peptide is in its charged form. As a sensitive parameter, we chose the phase-transition temperature of DMPC bilayer, which decreases by 4 °C in the presence of the completely charged form of $(LA)_{12}$. We chose the convenient and easy way to neutralize the positive charge of lysine groups—by raising the pH. The pK_a value for lysine amino groups in water is 10.5. However, in the presence of lipid bilayer membranes the apparent pK_a can be significantly changed. This change can be as high as a few pH units [41]. It was not surprising that at high pH the effect of $(LA)_{12}$ on the phase-transition temperature is significantly smaller. The phase-transition temperature of DMPC is shifted only by 1.6 °C at pH 9.5 and not affected at pH 11.5, indicating a weaker effect of the less charged and uncharged form of $(LA)_{12}$. Additionally, midpoints of the change of the effect of $(LA)_{12}$ on the phase-transition temperature appeared at pH 8.6 and ~10.9 indicating the apparent pK_as for lysine amino groups in the lipid bilayer. We refrained from investigating the effects of $(LA)_{12}$ on DMPC membrane properties at pH 11.5 and higher, where we expected to have a completely uncharged form of the peptide, because of membrane chemical

instability and oxygen consumption by unknown reactions that occur at pH extremes. We performed our experiment at pH 9.5. Our results indicate that at this pH the dilysine termini possess only one positive charge, as compared to two positive charges at pH 7.0. We called this form of $(LA)_{12}$ semi-charged.

The weaker effect of the semi-charged form of $(LA)_{12}$ on the phase-transition temperature could be the result of peptide aggregation, or the semi-charged form of $(LA)_{12}$ itself could affect the membrane differently than its charged from. To separate these possibilities we compared effects of $(LA)_{12}$ on membrane properties, such as the order and the rotational motion of alkyl chains, and an oxygen transport parameter, measured at pH 7.0, with those measured at pH 9.5. Neutralization of one positive charge of dilysine termini decreases the ordering effect of $(LA)_{12}$ by about 50%, which can be compared with the similar decrease of the effect on the phase-transition temperature. Formation of dimers and small oligomers which remove a certain amount of peptide from the interaction with lipid molecules can explain these effects. However, the semi-charged form of $(LA)_{12}$ decreases rotational motion of alkyl chains almost as effectively as the charged form (this effect changes with temperature) and their effects on oxygen transport parameter are the same. These findings weaken the possibility of formation of dimers and small oligomers of the semi-charged form of $(LA)_{12}$ but do not rule it out completely. The lifetime of transient oligomers may be of the order of 0.1 μs (thus they will not be detected by saturation-recovery EPR), but if about 50% of peptide molecules are in dimeric or greater oligomeric forms at any instant, the effects of the peptide on phospholipids will be reduced.

The strongest evidence against stable aggregation of the semi-charged form of $(LA)_{12}$ is the observation of the mono-exponential saturation–recovery signals of phosphatidylcholine spin labels in the absence and presence of molecular oxygen for DMPC-$(LA)_{12}$ membranes. Our saturation–recovery measurements, which are sensitive to time scales longer than approximately 0.5 μs (the shortest T_1 measured in the present experiments for 16-PC and 50% air), indicate that all of the phosphatidylcholine spin labels used in the present study detected a homogeneous environment in this time scale. This suggests that in the time scale of 0.5 μs, each lipid probe sampled virtually all of the microenvironment in the reconstituted membrane, including the position next to the peptide (monomeric or oligomeric), possibly the site sandwiched between two peptides, and the location away from the peptide. Regarding the sites directly in contact with two peptides, the number of such sites may be limited, and thus the lipids between the two peptides may not be detectable under the present conditions, or the lifetime of the oligomeric peptides (which could include lipids within the oligomeric complex) may be shorter than 0.5 μs. In the time scale of 0.5 μs, membrane components may be mixed. However, there is a good possibility that in the time scale of conventional EPR spectroscopy of ~10 ns, there may be (at least) two different environments. The absence of the second, more immobilized component in the conventional EPR spectra may be the result of the lack of sensitivity to detect such a component. We would like also to direct readers to the paper by Ashikawa et al. [46] where we showed that saturation–recovery method, and measurements of the oxygen collision rate, cannot differentiate the bulk and the protein-boundary domains, but they can differentiate between protein-clustered domain (or protein-rich domain) and the bulk-plus-boundary region. We should state here that our discussion is valid only for liquid-crystalline phase membranes for which the saturation–recovery experiments were performed. It was already shown that neutral WALP peptides, which are well dispersed in the liquid-crystalline phase PC membranes [34], form highly ordered striated domains when incorporated into the gel-phase PC bilayer [48].

It is surprising that the fully charged form of $(LA)_{12}$ (two positive charges et each end of the peptide) causes a much stronger effect not only on membrane phase transition but also on membrane order than the semi-charged form (one positive charge et each end of the peptide). It seems obvious that adding two positive charges to the moiety located between phosphatidylcholine headgroups of PC membranes should affect the interaction of these groups to a greater extent than adding one positive charge. Close interaction between the positively charged groups of $(LA)_{12}$ is unfavorable because of electrostatic repulsion. Additionally, this repulsion should be greater for the gel phase, since the charge density is larger than in the liquid-crystalline phase. This explains the different effect of charged and semi-charged forms of $(LA)_{12}$ on phase transition. Because of the repulsion of positive charges, the charged form of $(LA)_{12}$ should form a more evenly distributed lattice within the lipid bilayer in which peptides cannot approach each other too closely. Repulsion of peptide ends on both sides of the membrane should also better order the peptide molecules (make them more perpendicular to the membrane surface) and decrease the amplitude of their wobbling motion. It appears that the repulsion of peptide ends on both sides of the membrane decrease significantly when the charge at the end decreases from two to one. With this weaker repulsion barrier, the semi-charged form of $(LA)_{12}$ can diffuse and wobble more freely in the lipid bilayer, inducing less membrane order.

Acknowledgments

This work was supported by grants EY015526, and EB001980 of the NIH. We thank Dr. Joy Joseph for helpful conversations.

References

[1] A. Kusumi, Y. Sako, Cell surface organization by the membrane skeleton, Curr. Opin. Cell Biol. 8 (1996) 566–574.
[2] A. Kusumi, I. Koyama-Honda, K. Suzuki, Molecular dynamics and interactions for creation of stimulation-induced stabilized rafts from small unstable steady-state rafts, Traffic 5 (2004) 213–230.
[3] J.A. Killian, Hydrophobic mismatch between proteins and lipids in membranes, Biochim. Biophys. Acta 1376 (1998) 401–416.
[4] R.N.A.H. Lewis, Y.-P. Zhang, F. Liu, R.N. McElhaney, Mechanisms of the interaction of α-helical transmembrane peptides with phospholipid bilayers, Bioelectrochem. 56 (2002) 135–140.

[5] J.H. Davis, D.M. Clare, R.S. Hodges, M. Bloom, Interaction of a synthetic amphiphilic polypeptide and lipids in a bilayer structure, Biochemistry 22 (1983) 5298–5305.
[6] J.C. Huschilt, B.M. Millman, J.H. Davis, Orientation of alpha-helical peptides in a lipid bilayer, Biochim. Biophys. Acta 979 (1989) 139–141.
[7] E.J. Bolen, P.W. Holloway, Quenching of tryptophan fluorescence by brominated phospholipids, Biochemistry 29 (1990) 9638–9643.
[8] Y.-P. Zhang, R.N.A.H. Lewis, R.S. Hodges, R.N. McElhaney, FTIR spectroscopic studies of the conformation and amide hydrogen exchange of a peptide model of the hydrophobic transmembrane α-helices of membrane proteins, Biochemistry 31 (1992) 11572–11578.
[9] Y.-P. Zhang, R.N.A.H. Lewis, R.S. Hodges, R.N. McElhaney, Interaction of a peptide model of a hydrophobic transmembrane α-helical segment of a membrane protein with phosphatidylcholine bilayers: differential scanning calorimetry and FTIR spectroscopic studies, Biochemistry 31 (1992) 11579–11588.
[10] Y.-P. Zhang, R.N.A.H. Lewis, R.S. Hodges, R.N. McElhaney, Interaction of a peptide model of a hydrophobic transmembrane α-helical segment of a membrane protein with phosphatidylethanolamine bilayers: differential scanning calorimetry and FTIR spectroscopic studies, Biophys. J. 68 (1995) 847–857.
[11] P.H. Axelsen, P.H. Kaufman, R.N. McElhaney, R.N.A.H. Lewis, The infrared dichroism of transmembrane helical polypeptides, Biophys. J. 69 (1995) 2770–2781.
[12] W.K. Subczynski, R.N.A.H. Lewis, R.N. McElhaney, R.S. Hodges, J.S. Hyde, A. Kusumi, Molecular organization and dynamics of 1-palmitoyl-2-oleoylphosphatidylcholine bilayers containing a transmembrane α-helical peptide, Biochemistry 37 (1998) 3156–3164.
[13] R.N.A.H. Lewis, Y.-P. Zhang, R.S. Hodges, W.K. Subczynski, A. Kusumi, C.R. Flach, R. Mendelsohn, R.N. McElhaney, A polyamine-based peptide cannot form a stable transmembrane α-helix in fully hydrated phospholipids bilayer, Biochemistry 40 (2001) 12103–12111.
[14] W.K. Subczynski, M. Pasenkiewicz-Gierula, R.N. McElhaney, J.S. Hyde, A. Kusumi, Molecular dynamics of 1-palmitoyl-2-oleoylphosphatidylcholine membranes containing transmembrane α-helical peptides with alternating leucine and alanine residues, Biochemistry 42 (2003) 3939–3948.
[15] C. Paré, M. Laflear, F. Liu, R.N.A.H. Lewis, R.N. McElhaney, Differential scanning calorimetry and ^{2}H-nuclear magnetic resonance and Fourier transform infrared spectroscopy studies of the effects of transmembrane α-helical peptides on the organization of phosphatidylcholine bilayers, Biochim. Biophys. Acta 1511 (2001) 60–73.
[16] F. Liu, R.N.A.H. Lewis, R.S. Hodges, R.N. McElhaney, A differential scanning calorimetric and ^{31}P-NMR spectroscopic study of the effect of transmembrane α-helical peptides on the lamellar/reversed hexagonal phase transition of phosphatidyl-ethanolamine model membranes, Biochemistry 40 (2001) 760–768.
[17] F. Liu, R.N.A.H. Lewis, R.S. Hodges, R.N. McElhaney, Effect of variations in the structure of a polyleucine-based α-helical transmembrane peptide on its interaction with phosphatidylcholine bilayers, Biochemistry 41 (2002) 9197–9207.
[18] F. Liu, R.N.A.H. Lewis, R.S. Hodges, R.N. McElhaney, Effect of variations in the structure of a polyleucine-based α-helical transmembrane peptide on its interaction with phosphatidylglycerol bilayers, Biochemistry 43 (2004) 3679–3687.
[19] F. Liu, R.N.A.H. Lewis, R.S. Hodges, R.N. McElhaney, Effect of variations in the structure of a polyleucine-based α-helical transmembrane peptide on its interaction with phosphatidylethanolamine bilayers, Biophys. J. 87 (2004) 2470–2482.
[20] Y.-P. Zhang, R.N.A.H. Lewis, G.D. Henry, B.D. Sykes, R.S. Hodges, R.N. McElhaney, Peptide models of helical hydrophobic transmembrane segments of membrane proteins: I. Studies of the conformation, intrabilayer orientation and amide hydrogen exchangeability of Ac-K_2-$(LA)_{12}$-K_2-amide, Biochemistry 34 (1995) 2348–2361.
[21] Y.-P. Zhang, R.N.A.H. Lewis, R.S. Hodges, R.N. McElhaney, Peptide models of helical hydrophobic transmembrane segments of membrane proteins: II. DSC and FTIR spectroscopic studies of the interaction of Ac-K_2-$(LA)_{12}$-K_2-amide with phosphatidylcholine bilayers, Biochemistry 34 (1995) 2362–2371.
[22] Y.-P. Zhang, R.N.A.H. Lewis, R.S. Hodges, R.N. McElhaney, Peptide models of helical hydrophobic transmembrane segments of membrane proteins: interactions of acetyl-K_2-$(LA)_{12}$-K_2-amide with phosphatidylethanolamine bilayers, Biochemistry 40 (2001) 474–482.
[23] J.S. Hyde, W.K. Subczynski, Spin-label oximetry, in: L.J. Berliner, J. Reuben (Eds.), Biological Magnetic Resonance, Spin Labeling: Theory and Applications, vol. 8, Plenum Press, New York, 1989, pp. 399–425.
[24] W.K. Subczynski, J.S. Hyde, The diffusion-concentration product of oxygen in lipid bilayers using the spin-label T_1 method, Biochim. Biophys. Acta 643 (1981) 283–291.
[25] A. Kusumi, W.K. Subczynski, J.S. Hyde, Oxygen transport parameter in membranes as deduced by saturation recovery measurements of spin-lattice relaxation times of spin labels, Proc. Natl. Acad. Sci. U. S. A. 79 (1982) 1854–1858.
[26] W.K. Subczynski, J.S. Hyde, A. Kusumi, Oxygen permeability of phosphatidylcholine–cholesterol membranes, Proc. Natl. Acad. Sci. U. S. A. 86 (1989) 4474–4478.
[27] A. Wisniewska, Y. Nishimoto, J.S. Hyde, A. Kusumi, W.K. Subczynski, Depth dependence of the perturbing effect of placing a bulky group (oxazoline ring spin labels) in the membrane on the membrane phase transition, Biochim. Biophys. Acta 1278 (1996) 68–72.
[28] J.-J. Yin, M. Pasenkiewicz-Gierula, J.S. Hyde, Lateral diffusion of lipids in membranes by pulse saturation recovery electron spin resonance, Proc. Natl. Acad. Sci. U. S. A. 79 (1987) 1854–1858.
[29] K. Kawasaki, J.-J. Yin, W.K. Subczynski, J.S. Hyde, A. Kusumi, Pulse EPR detection of lipid exchange between protein-rich raft and bulk domains in the membrane: methodology development and its application to studies of influenza viral membrane, Biophys. J. 80 (2001) 738–748.
[30] J.-J. Yin, W.K. Subczynski, Effects of lutein and cholesterol on alkyl chain bending in lipid bilayers: a pulse electron spin resonance spin labeling study, Biophys. J. 71 (1996) 832–839.
[31] W.K. Subczynski, J.S. Hyde, A. Kusumi, Effect of alkyl chain unsaturation and cholesterol intercalation on oxygen transport in membranes: a pulse ESR spin labeling study, Biochemistry 30 (1991) 8578–8590.
[32] D.A. Windrem, W.Z. Plachy, The diffusion-solubility of oxygen in lipid bilayers, Biochim. Biophys. Acta 600 (1980) 655–665.
[33] K.P. Pauls, A.L. MacKay, O. Soderman, M. Bloom, A.K. Tanjea, R.S. Hodges, Dynamic properties of the backbone of an integral membrane polypeptide measured by 2H-NMR, Euro. Biophys. J. 12 (1985) 1–11.
[34] M.R. de Planque, D.V. Greathouse, R.E. Koeppe II, H. Schafer, D. Marsh, J.A. Killian, Influence of lipid/peptide hydrophobic mismatch on the thickness of diacylphosphatidylcholine bilayers. A ^{2}H NMR and ESR study using designed transmembrane alpha-helical peptides and gramicidin A, Biochemistry 37 (1998) 9333–9345.
[35] C. Huang, J.R. Lapides, I.W. Levin, Phase-transition behavior of saturated, symmetric chain phospholipid bilayer dispersions determined by Raman spectroscopy: correlation between spectral and thermodynamic parameters, J. Am. Chem. Soc. 104 (1982) 5926–5930.
[36] S. Mabrey, J.M. Sturtevant, Investigation of phase transitions of lipids and lipid mixtures by high sensitivity differential scanning calorimetry, Proc. Natl. Acad. Sci. U. S. A. 73 (1976) 3862–3866.
[37] J. Fumero, B.P. Bammel, H.P. Hopkins, J.C. Smith, The effect of potential-sensitive molecular probes on the thermal phase transition in dimyristoylphosphatidylcholine preparations, Biochim. Biophys. Acta 944 (1988) 164–176.
[38] H. Träuble, The movement of molecules across lipid membranes: a molecular theory, J. Membr. Biol. 4 (1971) 193–208.
[39] D. Papahadjopoulos, Surface properties of acidic phospholipids: interaction of monolayers and hydrated liquid crystals with uni- and bi-valent metal ions, Biochim. Biophys. Acta 163 (1968) 240–254.
[40] A. Kusumi, W.K. Subczynski, M. Pasenkiewicz-Gierula, J.S. Hyde, H. Merkle, Spin-label studies on phosphatidylcholine–cholesterol membranes: effects of alkyl chain length and unsaturation in the fluid phase, Biochim. Biophys. Acta 854 (1986) 307–317.

[41] H. Chaimovich, R.M.V. Aleixo, I.M. Cuccovia, D. Zanette, F.H. Quina, in: E.J. Fendler, K.L. Mittal (Eds.), Solution Behavior of Surfactants—Theory and Applied Aspects, vol. 2, Plenum Press, New York, 1982, pp. 949–974.
[42] D. Marsh, Electron Spin Resonance: Spin Labels, in: E. Grell (Ed.), Membrane Spectroscopy, Springer-Verlag, Berlin, 1981, pp. 51–142.
[43] A. Kusumi, M. Pasenkiewicz-Gierula, Rotational diffusion of steroid molecule in phosphatidylcholine membranes: effects of alkyl chain length, unsaturation, and cholesterol as studied by a spin-label method, Biochemistry 27 (1988) 4407–4415.
[44] B. Gafney, Practical considerations for the calculations of order parameters for fatty acid or phospholipid spin labels in membranes, in: L.J. Berliner (Ed.), Spin Labeling. Theory and Applications, Academic Press, New York, 1976, pp. 567–571.
[45] L.J. Berliner, Spin labeling in enzymology: spin-labeled enzymes and proteins. (Rotational correlation times calculation), Methods Enzymol. 49 (1978) 466–470.
[46] I. Ashikawa, J.-J. Yin, W.K. Subczynski, T. Kouyama, J.S. Hyde, A. Kusumi, Molecular organization and dynamics in bacteriorhodopsin-rich reconstituted membranes: discrimination of lipid environments by the oxygen transport parameter using a pulse ESR spin-labeling technique, Biochemistry 33 (1994) 4947–4952.
[47] W.K. Subczynski, A. Kusumi, Dynamics of raft molecules in cellular and artificial membranes: approaches by pulse EPR spin labeling and single molecule optical microscopy, Biochim. Biophys. Acta 1610 (2003) 231–243.
[48] E. Sparr, D.N. Ganchev, M.M.E. Snel, A.N.J.A. Ridder, L.M.J. Kroon-Batenburg, V. Chupin, D.T.S. Rijkers, J.A. Killian, B. de Kruijff, Molecular organization in striated domains induced by transmembrane α-helical peptides in dipalmitoyl phosphatidylcholine bilayers, Biochemistry 44 (2005) 2–10.